Geomechanics and Engineering, *Vol. 35, No. 2 (2023) 181-194*
https://doi.org/10.12989/gae.2023.35.2.181

Effect of cross-section geometry on the stability performance of functionally graded cylindrical imperfect composite structures used in stadium construction

Ying Yang[1] and Yike Mao*[2]

[1]*College of Universal Quality Education, Wuchang University of Technology, Wuhan 430223, Hubei, China*
[2]*Department of Physical Education, Wuhan University of Technology, Wuhan 430076, Hubei, China*

(*Received March 3, 2023, Revised August 30, 2023, Accepted September 4, 2023*)

Abstract. The primary objective of this study is to examine the influence of geometry on the stability characteristics of cylindrical microstructures. This investigation entails a stability analysis of a bi-directional functionally graded (BD-FG) cylindrical imperfect concrete beam, focusing on the impact of geometry. Both the first-order shear deformation beam theory and the modified coupled stress theory are employed to explore the buckling and dynamic behaviors of the structure. The cylinder-shaped imperfect beam is constructed using a porosity-dependent functionally graded (FG) concrete material, wherein diverse porosity voids and material distributions are incorporated along the radial axis of the beam. The radius functions are considered in both uniform and nonuniform variations, reflecting their alterations along the length of the beam. The combination of these characteristics leads to the creation of BD-FG configurations. In order to enable the assessment of stability using energy principles, a numerical technique is utilized to formulate the equations for partial derivatives (PDEs).

Keywords: buckling analysis; concrete beam; functionally graded material; nonlinear analysis; porous material; truncated conical tube

1. Introduction

In the pursuit of developing a composite substance that harmonizes the traits of varied materials within a unified structure, an innovative genre of composite arrangement, recognized as functionally graded materials (FGMs), is meticulously fashioned. These FGMs are built using different phases of materials that vary in a specific direction without distinct boundaries. For instance, an FGM comprising ceramics in addition to carbon steel can exhibit the flexibility of steel along with the thermal properties inherent in ceramics. As a result, this type of material can withstand higher temperatures and mitigate both thermal and mechanical stresses within a structure, without posing any safety concerns compared to homogeneous materials. Consequently, FGMs, due to their diverse properties, have captured the attention of numerous scholars (Cheng *et al.* 2023, Guo *et al.* 2023, Huang *et al. 2*023b, Tang *et al. 2*023, Wu *et al.* 2023a, Zhao *et al. 2*023). Extensive research has been dedicated to comprehending the thermal attributes of functionally graded materials (FGMs), placing a specific focus on their conductive behaviors concerning heat across varying shapes and scenarios. Notably, Amiri Delouei *et al. (*2019a) stands out for its significant advancements. It has contributed by presenting analytical solutions in closed form, specifically addressing the realm of axisymmetric heat conduction within finite functionally graded cylinders. Additionally, their research delves into the domain of two-dimensional uneven heat conduction within segments of cylindrical FGMs (Amiri Delouei *et al. 2*019b). Moreover, the team introduced a comprehensive analytical approach to tackle the intricate temperature distribution in functionally graded hollow spheres, while accounting for a wide spectrum of thermal boundary conditions (Amiri Delouei *et al.* 2020). Extending their investigations, the researchers explored the intricate domain of non-uniform heat conduction in boundless functionally graded cylinders. Their findings culminated in a meticulously derived, precise two-dimensional analytical solution that holds relevance across diverse boundary conditions (Delouei *et al.* 2020). In a parallel vein of contribution, Emamian *et al. (*2021) have also significantly enriched this domain. Their work introduces an analytical solution for the transfer of heat in cones crafted from functionally graded material, while simultaneously delving into the intricate landscape of irregular temperature distribution within cylinders constituted of functionally graded materials under boundary conditions involving convective heat transfer with circumferential variation (He *et al.* 2023). These collective endeavors substantially deepen our comprehension of the thermal attributes intrinsic to FGMs and their far-reaching implications across diverse practical applications (Cai *et al. 2*023, Huang *et al.* 2023a, Li *et al.* 2023a, Li *et al. 2*023b, Li *et al.* 2023c).

For the advancement of technologies like actuators, sensors, and energy harvesters, a fundamental requirement emerged – the scrutiny of the flexural and buckling traits exhibited by diminutive structures (Omidi *et al. 2*013, Ghadiri *et al.* 2016c, Mousavi *et al. 2*017). A significant aspect to take into account is that the enhancement of energy harvesting and the efficacy of sensing could be

*Corresponding author, Ph.D.
E-mail: 269268@whut.edu.cn

ISSN: 2005-307X (Print), 2092-6219 (Online)

achieved through phenomena such as finite disturbance buckling, bifurcation, and snap-through transitions. These mechanisms can effectively convert low-rate excitation into the responsive motion of devices, facilitated by piezoelectric transducers (Azimi *et al. 2*016, Ghadiri *et. al.* 2016a, Ghadiri *et al. 2*016b, Shafiei *et al.* 2016, Shafiei *et al.* 2017). Microstructures, which find applications in creating devices such as micro-fluid-flow controllers, energy harvesters, atomic force microscopes, microelectromechanical systems (MEMS), microsensors, and microswitches, represent a crucial area of exploration for researchers. Consequently, it is imperative to acknowledge that classical continuum theories are inadequate for comprehensively investigating these structures, as evidenced by experimental studies. In response, scholars have endeavored to propose novel elasticity theories that allow for the examination of behaviors inherent to these diminutive structures (Mohammadi *et al. 2*020, Wang *et al.* 2020a, Ugurlu and Ozturk 2021, Dehghanbanadaki *et al. 2*022, Wang *et al.* 2023b). An influential theory in this context is the modified couple stress theory (MCST), introduced by Yang *et al.* (2002), which enables the exploration of small-scale properties of such structures. This theory's reliability was substantiated through experimental investigations, leading many researchers to adopt this elasticity framework for modeling and analyzing the behaviors of small-scaled and thin-walled structures (Kim *et al.* 2019).

The microtubes which are made by FG materials play a significant role in MEMS devices. Thus, the investigation in which these structures are utilized have been raised in the past few years. Regarding this, Ghannadpour and Mohammadi (2010) modeled a microtube based on Timoshenko beam theory to investigate its buckling. The formulation in this article was solved via Rayleigh-Ritz method. Akgöz and Civalek (2011) conducted a study where they employed Monte Carlo simulation (MCS) in conjunction with the strain gradient theory. Their focus was on examining the buckling response exhibited by a nanotube that is cantilevered in nature. Li and Hu (2015), analytically examined the nonlinear buckling response of nanobeams using classical as well as strain gradient theories. In another paper, the mechanical response of a microtubule was analyzed via buckling examination by Kabir *et al.* (2015). Xiang and Liew (2011) examined the static response associated with a microtubule via higher-order gradient as well as atomistic continuum theories. In the study by Farajpour *et al.* (2019), a comprehensive analysis was conducted, encompassing both the buckling behavior and the subsequent post-buckling response of microtubes engineered for fluid conveyance.

Because of the problem in the process of making tubes and beams, forming micro-tubes/-beams with non-uniform-cross section is a common phenomenon (Liu *et al. 2*020, Wang *et al. 2*020b, Zhou *et al. 2*020, Dai *et al.* 2021,Guo *et al.* 2021, Shao *et al. 2*021; Wu and Habibi 2021). Additionally, in other cases, these nonuniform tubes are made deliberately to be utilized as fluid flow throat, fluid flow nozzle, thermal fin, and fluid flow diffuser (Ehyaei *et al.* 2017, Ghadiri *et al. 2*017a, Ghadiri *et al. 2*017b, Shivanian *et al. 2*017). It is vital to be remembered that this nonuniformity can affect the mechanical behavior of such structures. In this regard, there are various studies in which, by considering the effect of small size, the influence of these nonuniformities is investigated. However, these structures, because of their quite complex formulation, has not been studied widely. Jiao *et al.* (2016) studied the buckling response related to different beams with different shape for their cross section. Additionally, based on FSDT, the buckling associated with tapered beams which are made of AFGM was studied by Huang *et al.* (2016).

Additionally, there are different studies in which the thermoelastic impact on the mechanical performance of systems has been examined (Ebrahimi *et al.* 2017, Ghadiri *et al.* 2017c, Shahabinejad *et al.* 2018, Shafiei *et al.* 2020). Accordingly, Raoofian Naeeni *et al.* (2013), by using Hankel as well as Laplace integral transforms, solved the formulation related to thermoelastic materials. The coupled equations associated thermoelastic Half-Space was uncoupled in six different equations and solved with the help of Hankel transformation by Hayati *et al.* (2013). Also, the temperature, stress, as well as displacement of a thermoelastic half-space which is subjected to heat flux in addition to axisymmetric vertical traction was studied (Yang *et al.* 2019, Wu *et al.* 2022, Wang *et. al.* 2023a, Wu *et al.* 2023b, Yang *et al.* 2023). In addition, the Green's functions identified a half-space including a thermoviscoelastic layer and a thermoelastic layer was attained by Naeeni *et al.* (2015). The wave multiplication of a homogenous half-space was explored by Hayati and Eskandari-Ghadi (2018). In the aforementioned article, the temperature, stress, as well as displacement was acquired via Biot's formulations. four scalar functions was presented in order to decouple the formulation between temperature and displacements based on nonclassical Lord–Shulman equations (Hou *et al.* 2021b, Huang *et al.* 2021, Xu *et al.* 2021, Wang *et al.* 2022). Four couple formulation for a three-dimensional wave propagation in isotopic thermoelastic materials was reduced to two PDE by Hayati *et al.* (2021). The formulation associated with temperature, stress, as well as displacement of a thermoelastic solid which was subjected to heat flux in addition to mechanical loading was presented (Yang *et al.* 2022, Yao *et al.* 2023, Yu *et al.* 2023, Zhang 2023, Zhou *et al.* 2023). The communication between the beneath soil as well as the network was analyzed through the finite element model. Also, the structure in this paper was under seismic waves as well as external forces.

This research paper introduces a comprehensive investigation into an important and previously underexplored aspect of microstructure behavior. However, like any scientific inquiry, this study has its limitations. The analysis primarily focuses on a specific type of bi-directional functionally graded cylindrical beams, and while this provides valuable insights, it might not encompass the full spectrum of diverse geometries and configurations present in practical applications. Additionally, the utilization of theoretical models and numerical methods, while essential for analytical precision, might not capture all the intricacies of real-world scenarios, leading to some degree of approximation. Nonetheless, this research acts as a vital

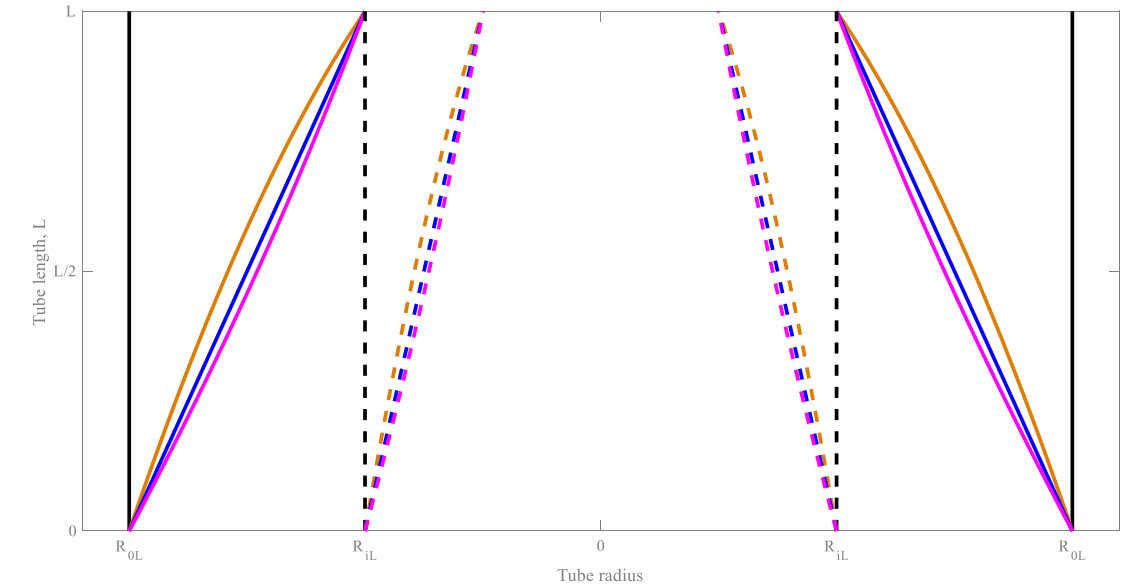

(a)

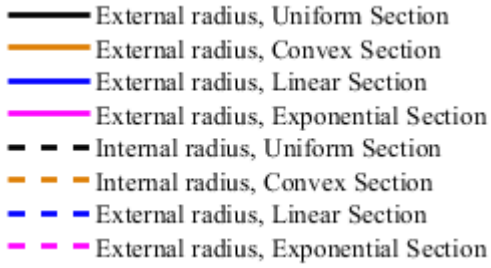

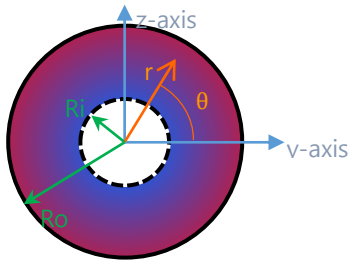

(b)

Fig. 1 (a) Different radius funcion for uniform exponential, convex and linear section, (Ro=2Ri) and (b) geometry as well as coordinated related to FG nanotube

bridge between the realms of geometry and stability in functionally graded microstructures. By systematically examining the influence of cross-sectional geometry on stability, this work sheds light on a previously unexplored interaction and provides a foundation for further investigations. The novelty of the study lies in its approach to merging geometry and stability in functionally graded structures, offering a new dimension to the understanding of these materials. The practical implications of this manuscript are vast, with potential applications in various engineering fields, including actuators, sensors, and energy harvesters. The insights gained from this research could pave the way for optimized designs, improved performance, and enhanced functionality of cylindrical microstructures, ultimately contributing to advancements in engineering applications and materials science.

Moving on to the specific research focus, the paper delves into the nonlinear buckling behavior of functionally graded concrete microtubes featuring various cross-sectional shapes, while considering the presence of porosity. The formulation of the problem is established using the von-Kármán theory and incorporates the modified couple stress (MCS) approach. The article proceeds with a structured approach: firstly, formulating the nonlinear buckling problem for microtubes using the energy method, addressing both uniform and nonuniform FG tubes. Following this, the utilization of the Generalized Differential Quadrature Method (GDQM) in conjunction with an iterative technique comes into play for the acquisition of both linear and nonlinear outcomes. In the conclusive stage, the proposed methodology and the resultant equations are subjected to validation, while the influence of varying parameters on the buckling behavior of functionally graded microbeams is meticulously examined.

2. Mathematics of the problem

Fig. 1 illustrates a microtube composed of functionally graded (FG) materials, characterized by the parameters L, Ri, and Ro, representing its length, inner radius, and outer radius, respectively. The FG tube is comprised of two distinct sections: an internal surface constructed from metal and an external surface made from concrete. The material between these two sections exhibits variations described by four distinct functions. The cross-sectional uniformity or nonuniformity of the tube is considered, along with alterations in thickness based on both nonlinear and linear

functions, which are specified by the subsequent equations.

$$R\left(x\right)=R_L\left(1-\beta\frac{x}{L}\right)^{Rn} \tag{1a}$$

$$R\left(x\right)=R_L e^{-\left(\xi\frac{x}{L}\right)} \tag{1b}$$

In these equations, 'ζ', 'β', and 'R_L' represent non-zero parameters, these factors pertain to the speed at which the cross-sectional shape alters and the initial diameter of the tube (at x=0), respectively. Moreover, 'Rn' serves as a factor that determines the cross-sectional shape of the tube. Specifically, for uniform, convex, and linear sections, 'Rn' corresponds to 0, 0.5, and 1, respectively. Notably, the functions of 'R' can be applied to both the outer and inner radii. Additionally, Eq. ((1(b)) characterizes the function associated with the exponential section.

The material chosen for this study is a functionally graded substance composed of metal and concrete on the two opposing facets of the tube. The intermediary material showcases a seamless transition lacking distinctive boundaries. Consequently, the Poisson's ratio (v) and Young's modulus (E) connected with this material are outlined as follows.

$$\begin{aligned}&E\left(x,r\right)=\\&E_m+\left(E_c-E_m\right)\left(\frac{r-R_i\left(x\right)}{R_o\left(x\right)-R_i\left(x\right)}\right)^{px}-\\&\eta\cos\left(\frac{r-R_i\left(x\right)}{R_o\left(x\right)-R_i\left(x\right)}\frac{\pi}{2}\right)\times\\&\left[E_m+\left(E_c-E_m\right)\left(\frac{r-R_i\left(x\right)}{R_o\left(x\right)-R_i\left(x\right)}\right)\right]\end{aligned} \tag{2a}$$

$$\begin{aligned}&\nu\left(x,r\right)=\\&\nu_m+\left(\nu_c-\nu_m\right)\left(\frac{r-R_i\left(x\right)}{R_o\left(x\right)-R_i\left(x\right)}\right)^{px}-\\&\eta\cos\left(\frac{r-R_i\left(x\right)}{R_o\left(x\right)-R_i\left(x\right)}\frac{\pi}{2}\right)\\&\times\left[\nu_m+\left(\nu_c-\nu_m\right)\left(\frac{r-R_i\left(x\right)}{R_o\left(x\right)-R_i\left(x\right)}\right)\right]\end{aligned} \tag{2b}$$

In the context of these formulations, the notations "m" and "c" denote metal and concrete or ceramic correspondingly. Additionally, "px" signifies the power functionally graded index, while "Ri" and "Ro" are calculated using Eq. (1). The symbol "η" stands for the porosity coefficient. The material properties corresponding to various materials are outlined in Table 1.

In the current study, two coordinate systems, namely cylindrical and rectangular, are employed to formulate the problem. The following are the relationships between these two coordinate systems.

$$\left\{y\quad z\right\}=r\times\left\{\cos\left(\theta\right)\quad\sin\left(\theta\right)\right\} \tag{3}$$

Table 1 Young's modulus as well as Poisson's ratio of different metals, ceramics and concrete (Yang and Shen 2002, Tahmasebinia *et al.* 2022)

	ν	E (GPa)
SUS304	0.24	201.04
Al_2O_3	0.24	323.393
Nickel	0.31	205.097
Concrete	0.2	30
Steel	0.3	200

The formulation and end conditions are derived using the energy method. The energy method for buckling analysis is outlined as follows

$$\delta U+\delta W=0 \tag{4}$$

Within this framework, U represents the potential energy, whereas W pertains to external work. The displacements in the x, y, and z directions are characterized using the Timoshenko beam model, defined in the subsequent manner

$$u_1=u-r\sin\left(\theta\right)w_{,x} \tag{5a}$$

$$u_2=0 \tag{5b}$$

$$u_3=w \tag{5c}$$

Within this context, w(x) denotes the lateral deflection, and ∂w/∂x signifies the angular rotation. Through the utilization of the modified couple stress (MCS) theory, the interrelations connecting stress and strain, as initially introduced by Yang *et al.* (2002), can be formulated as follows

$$U=\frac{1}{2}\int\left(m:\chi+\sigma:\varepsilon\right)dV \tag{6}$$

In this context, ε represents strain, and σ signifies stress. Furthermore, m and χ indicate the symmetric curvature tensors and the deviatoric segment of the couple stress, correspondingly.

$$2\chi=\nabla\vartheta+\left(\nabla\vartheta\right)^T \tag{7}$$

Where

$$2\vartheta=curl\left(u\right) \tag{8}$$

Also, stresses are

$$\sigma=E\,\varepsilon \tag{9a}$$

$$m=2\chi\kappa l^2 \tag{9b}$$

The small-scale factor is denoted by "l" Furthermore, the Lamé constant is represented by κ. In accordance with von-Kármán's theory, where moderate rotation and significant transverse displacement are assumed, the

nonlinear strain-displacement relation can be formulated as follows

$$\varepsilon_{xx} = u_{,x} - r\sin(\theta)w_{,xx} + \frac{1}{2}w_{,x}^{2} \tag{10}$$

Based on the provided strain and stress components, the potential energy can be computed as follows

$$\begin{aligned}\delta U = &\int E u_{,x} w_{,x} \delta(w_{,x})\, dV \\ &+\int \kappa l^2 w_{,xx}\delta(w_{,xx})\, dV \\ &+\int \frac{1}{2}E(w_{,x})^2\delta(u_{,x})\, dV \\ &+\int E r^2 \sin^2(\theta) w_{,xx}\delta(w_{,xx})\, dV \\ &+\int \frac{1}{2}E w_{,x}^{3}\delta(w_{,x})\, dV + \int E u_{,x}\delta(u_{,x})\, dV\end{aligned} \tag{11}$$

Moreover, the energy associated with the external loads is calculated as follows

$$\delta W = \int \bar{F} w_{,x}\delta(w_{,x})\, dV \tag{12}$$

The load causing buckling is represented as $\bar{F}$. By inserting Eqs. (11) and (12) into Eq. (4), the Euler–Lagrange equation can be derived in the following manner

$$\delta(w): \frac{\partial^2\left(\varpi_1 l^2 w_{,xx} + \varpi_2 w_{,xx}\right)}{\partial x^2} = \frac{\partial}{\partial x}\left(\left[\varpi_3 u_{,x} + \frac{1}{2}\varpi_3(w_{,x})^2 - \bar{F}\right]\frac{\partial w}{\partial x}\right) \tag{13a}$$

$$\frac{\partial\left(\varpi_3 u_{,x} + \frac{1}{2}\varpi_3(w_{,x})^2 - \bar{F}\right)}{\partial x} = 0 \tag{13b}$$

where

$$\varpi_1 = \iint E(x,r)\frac{1}{2+2\nu(x,r)}\, r\, dr\, d\theta \tag{14a}$$

$$\varpi_2 = \iint E(x,r) r^3 \sin(\theta) dr\, d\theta \tag{14b}$$

$$\varpi_3 = \iint E(x,r)\, r\, dr\, d\theta \tag{14c}$$

Also, boundary conditions are

$$\delta(w): \varpi_1 l^2 w_{,xxx} + \varpi_2 w_{,xxx} + \frac{d\varpi_1}{dx} l^2 w_{,xx} + \frac{d\varpi_2}{dx} w_{,xx} = 0 \tag{15a}$$

$$\delta(w_{,x}): \varpi_1 l^2 w_{,xx} + \varpi_2 w_{,xx} = 0 \tag{15b}$$

$$\delta(u): \varpi_3 u_{,x} + \frac{1}{2}\varpi_3(w_{,x})^2 = 0 \tag{15c}$$

3. Numerical solution method

This paper employs a numerical approach known as the Generalized Differential Quadrature Method (GDQM) to compute the linear and nonlinear partial differential equations. In the GDQM, the derivatives of functions with different orders are transformed into matrices. This method provides a systematic way to discretize the differential equations, allowing for the efficient solution of complex mathematical problems. Through the utilization of matrices to express the derivatives, the initial differential equations undergo a conversion into algebraic equations that can be effectively addressed using matrix operations. The Generalized Differential Quadrature Method (GDQM) has demonstrated its adaptability and efficacy in handling diverse sets of differential equations, particularly in scenarios encompassing intricate geometries, material attributes, and boundary prerequisites. This approach enhances the accuracy and computational efficiency of solving partial differential equations, making it a valuable tool for analyzing the behavior of microstructures in various engineering applications. Here, the υ-order derivative function of '*f*' according to the GDQM is formulated as follows

$$\left.\frac{\partial^{\upsilon} f(x)}{\partial x^{\upsilon}}\right|_{x=x_j} = \sum_{j=1}^{n}\Theta_{ij}^{(\upsilon)} f(x_i) \tag{16a}$$

In which *n* refer to grid points' number. Also, "Θ_{ij}" can be obtained

$$\Theta_{ij}^{(1)} = \frac{\Gamma(x_i)}{\Gamma(x_j)x_i - \Gamma(x_j)x_j} \tag{16b}$$

In which $\Xi(x)$ is

$$\Gamma(x_i) = \prod_{j=1, j\neq i}^{n}(x_i - x_j) \tag{16c}$$

Also, $\Theta^{(r)}$ can be attained through the following equations.

$$\Theta_{ij}^{(\upsilon)} = \upsilon\Theta_{ij}^{(r-1)}\Theta_{ij}^{(1)} - \upsilon\left(x_i - x_j\right)^{-1}\Theta_{ij}^{(r-1)} \tag{16d}$$

Additionally, the greed points are dispersed nonuniformly as follows.

$$x_i = \frac{1}{2} - \frac{1}{2}\cos\left(\pi(i-1)(n-1)\right) \tag{16e}$$

The matrices format of the governing equations according to the GDQM are presented as follows

$$\begin{bmatrix}[K_1] & [K_2]\\ [K_3] & [K_4]\end{bmatrix}_{Nonlinear}\begin{Bmatrix}u\\ w\end{Bmatrix} + \begin{bmatrix}[K_5] & [K_5]\\ [K_7] & [K_8]\end{bmatrix}_{Linear}\begin{Bmatrix}u\\ w\end{Bmatrix} = \bar{F}\begin{bmatrix}[M_1] & [M_2]\\ [M_3] & [M_4]\end{bmatrix}\begin{Bmatrix}u\\ w\end{Bmatrix} \tag{17a}$$

where

$$[K_1]=\frac{d\varpi_3}{dx}\frac{\partial u}{\partial x}+\varpi_3\frac{\partial^2 u}{\partial x^2} \tag{17b}$$

$$[K_4]=\varpi_2 w_{,xxxx}+2\frac{d\varpi_3}{dx}w_{,xxx}+\frac{d^2\varpi_3}{dx^2}w_{,xx}+l^2\left(\frac{d^2\varpi_1}{dx^2}w_{,xx}+\varpi_1 w_{,xxxx}+2\frac{d\varpi_1}{dx}w_{,xxx}\right) \tag{17c}$$

$$[K_6]=\frac{1}{2}\varpi_3\frac{\partial}{\partial x}\left(w_{,x}\right)^2+\frac{1}{2}\frac{d\varpi_3}{dx}\left(w_{,x}\right)^2 \tag{17d}$$

$$[-K_7]=\varpi_3 u_{,x}w_{,xx}+\varpi_3 w_{,x}u_{,xx}+\frac{d\varpi_3}{dx}u_{,x}w_{,x} \tag{17e}$$

$$[-K_8]=\frac{1}{L}\varpi_3\frac{\partial}{\partial x}\left(\int_0^L\left(w_{,x}\right)^2dx\right)+\frac{1}{2L}\frac{d\varpi_3}{dx}\int_0^L\left(w_{,x}\right)^2dx+\frac{1}{2L}\varpi_3\int_0^L\left(w_{,x}\right)^2dx\,w_{,xx} \tag{17f}$$

$$[M_4]=w_{,xx} \tag{17g}$$

$$[K_2]=[K_3]=[K_5]=[M_1]=[M_2]=[M_3]=0 \tag{17h}$$

Moreover, the boundary prerequisites (Eqs. (15)) can similarly be rendered as a composite of three matrices. The procedure commences by excluding the nonlinear components within the stiffness matrix, ultimately resulting in the ensuing formulation. Moreover, through the utilization of derivative GDQ functions, the governing equations undergo transformation into the following expressions

$$\begin{aligned}&\delta(w):\\&+l^2\left(\begin{array}{l}\frac{d^2\varpi_1}{dx^2}\sum_{j=1}^{n}\Theta_{ij}^{(2)}w_i\\+\varpi_1\sum_{j=1}^{n}\Theta_{ij}^{(4)}w_i\\+2\frac{d\varpi_1}{dx}\sum_{j=1}^{n}\Theta_{ij}^{(3)}w_i\end{array}\right)\varpi_2\sum_{j=1}^{n}\Theta_{ij}^{(4)}w_i\\&-\frac{d\varpi_3}{dx}\sum_{j=1}^{n}\Theta_{ij}^{(1)}u_i\sum_{j=1}^{n}\Theta_{ij}^{(1)}w_i\\&+\frac{d^2\varpi_2}{dx^2}\sum_{j=1}^{n}\Theta_{ij}^{(2)}w_i+2\frac{d\varpi_2}{dx}\sum_{j=1}^{n}\Theta_{ij}^{(3)}w_i\\&+\varpi_3\sum_{j=1}^{n}\Theta_{ij}^{(1)}w_i\sum_{j=1}^{n}\Theta_{ij}^{(2)}u_i\\&-\frac{1}{2L}\varpi_3\int_0^L\left(\frac{\partial w}{\partial x}\right)^2dx\sum_{j=1}^{n}\Theta_{ij}^{(2)}w_i\\&-\varpi_3\sum_{j=1}^{n}\Theta_{ij}^{(1)}u_i\sum_{j=1}^{n}\Theta_{ij}^{(2)}w_i\\&-\left(\begin{array}{l}\frac{1}{2L}\frac{d\varpi_3}{dx}\int_0^L\left(\frac{\partial w}{\partial x}\right)^2dx\\+\frac{1}{L}\varpi_3\frac{\partial}{\partial x}\left(\int_0^L\left(\frac{\partial w}{\partial x}\right)^2dx\right)\end{array}\right)\sum_{j=1}^{n}\Theta_{ij}^{(1)}w_i\\&=\frac{d\bar{F}}{dx}\sum_{j=1}^{n}\Theta_{ij}^{(1)}w_i+\bar{F}\sum_{j=1}^{n}\Theta_{ij}^{(2)}w_i\end{aligned} \tag{18a}$$

$$\begin{aligned}&\delta(u):\varpi_3\sum_{j=1}^{n}\Theta_{ij}^{(2)}w_i\left(w_{,x}\right)\\&+\frac{d\varpi_3}{dx}\sum_{j=1}^{n}\Theta_{ij}^{(1)}u_i\frac{d\bar{F}}{dx}+\varpi_3\sum_{j=1}^{n}\Theta_{ij}^{(2)}u_i\\&+\frac{1}{2}\frac{d\varpi_3}{dx}\left(w_{,x}\right)\sum_{j=1}^{n}\Theta_{ij}^{(1)}w_i=0\end{aligned} \tag{18b}$$

The integration of the above-stated equations, combined with the boundary conditions detailed by the equation above and Eqs. (21), facilitates the determination of the linear buckling loads for a functionally graded microtube. This process is elucidated within the subsequent steps.

$$\begin{bmatrix}[K_{dd}] & [K_{db}]\\ [K_{bd}] & [K_{bb}]\end{bmatrix}_{Linear}\begin{Bmatrix}\{\lambda_d\}\\ \{\lambda_b\}\end{Bmatrix}=\bar{F}\begin{bmatrix}[M_{dd}] & [M_{db}]\\ [M_{bd}] & [M_{bb}]\end{bmatrix}\begin{Bmatrix}\{\lambda_d\}\\ \{\lambda_b\}\end{Bmatrix} \tag{19a}$$

Within this framework, the symbols 'd' and 'b' correspond to the domain and boundary, respectively. Moreover, the character 'λ' stands for the mode shape. The initial nonlinear buckling load can be derived by utilizing the eigenvalues obtained from Eq. (19) and subsequently identifying their corresponding mode shapes. These mode shapes are then integrated into the subsequent relation as the initial step within the solution.

$$\left(\begin{array}{l}\begin{bmatrix}[K_{dd}] & [K_{db}]\\ [K_{bd}] & [K_{bb}]\end{bmatrix}_{Non-linear}\\-\bar{F}_{nonlinear}\begin{bmatrix}[M_{dd}] & [M_{db}]\\ [M_{bd}] & [M_{bb}]\end{bmatrix}\\+\begin{bmatrix}[K_{dd}] & [K_{db}]\\ [K_{bd}] & [K_{bb}]\end{bmatrix}_{Linear}\end{array}\right)\begin{Bmatrix}\{\lambda_d\}\\ \{\lambda_b\}\end{Bmatrix}=0 \tag{19b}$$

Hence, the updated nonlinear outcomes can be acquired by employing the nonlinear mode shapes as outlined in Eq. (19). This iterative process persists until the results exhibit convergence, in accordance with the equation presented below.

$$error=\frac{\bar{F}_{i+1}-\bar{F}_i}{\bar{F}_{i+1}} \tag{19c}$$

In this scenario, the error value is set to 0.0001.

4. Numerical results and description

In this process, the Generalized Differential Quadrature Method (GDQM) is employed to establish nonlinear equations that pertain to imperfect microtubular beams made of functionally graded materials. These beams are subjected to clamped-pinned (C-P), fully pinned (P), or fully clamped (C) boundary conditions. Initially, the results obtained in the present study are compared with findings from existing literature, thus ensuring the validation of both the formulation and solution approach. Following this validation, the investigation proceeds to examine the influences of various factors on the buckling behavior of the microtube. These factors include the porosity coefficient,

Table 2 Buckling loads (FE_cI_0/L^2) of the presented study compared to Hou *et al*. (2021a)

	l/2Ro=0	*l*/2Ro=0.2	*l*/2Ro=0.4	*l*/2Ro=0.6	*l*/2Ro=0.8	*l*/2Ro=1.0
HPM, Hou *et al.* (2021a)	9.8696444	115.858121	167.348965	253.1795242	373.32875	527.8090211
GDQM, Hou *et al.* (2021a)	9.8696444	115.859003	167.3501245	253.1811254	373.33333	527.8096584
Present study, HPM	9.868657436	115.8465352	167.3322301	253.1542062	373.2914171	527.7562402
Present study, GDQM	9.868657436	115.8474171	167.3333895	253.1558073	373.2959967	527.7568774

Table 3 Nonlinear buckling loads (FE_cI_0/L^2) for a microbeam, px=1 (Al_2O_3/SUS304), η=0.2

	W/R=1			W/R=2		
	l/Ro=0.1	*l*/Ro=0.2	*l*/Ro=0.3	*l*/Ro=0.1	*l*/Ro=0.2	*l*/Ro=0.3
Shafiei and Kazemi (2017)	28.44483	32.26212	38.62422	32.06644	35.88641	42.25194
He and Cai (2021)	28.4450142	32.2622548	38.6243215	32.0669875	35.8869854	42.2521542
Present study	28.44216967	32.25902854	38.62045903	32.06378077	35.88339667	42.24792894

the power-law index parameter for functionally graded materials, nonlinearity, temperature, and different cross-sectional configurations. The subsequent equation introduces the concept of the nondimensional buckling load (F), the small-scale factor (μ), and the impact of large deflection (W/R).

$$l^2=\mu^2 Ro_L \tag{20a}$$

$$W/R=\bar{w}\sqrt{\frac{I_0}{A_0L^2}} \tag{20b}$$

$$F=\bar{F}\frac{\pi L^2}{Ec\times I_0} \tag{20c}$$

It is pertinent to acknowledge that the term "*Ec*" denotes the Young's modulus of concrete, while "*I0*" and "*A0*" represent the moment of inertia and cross-sectional area attributed to the left side of the microtube. Furthermore, "*R0o*" signifies the outer radius of the microtube, with the notation "$\bar{w}$" denoting the nonlinear large deflection inherent to the microtube. The validation of this study has been executed through the utilization of Table 2, which juxtaposes the outcomes of the present study against those of distinct scholarly works encompassing diverse boundary conditions. This tabular comparison underscores the veracity of both the formulation and the procedural approach adopted in scrutinizing the buckling behavior of micropipes.

This section addresses the scrutiny of several parameters to assess their influences on the buckling behavior of the tube, both in linear and nonlinear contexts. Notably, a configuration of Ro/Ri=2 and R_L/R_R=2 is upheld throughout. To ascertain the credibility of the nonlinear buckling load, Table 3 is presented. Within this tabular representation, the nonlinear buckling phenomena associated with an FG porosity-dependent microbeam ($SUS304/Al_2O_3$) are ascertained and juxtaposed with the findings of of He and Cai (2021) and Shafiei and Kazemi (2017). It is imperative to underscore that a cylindrical beam is being contrasted with a rectangular beam. Consequently, Eq. (2) is subsequently reformulated in the following manner. Table 3 demonstrates the credibility and accuracy of the formulation in extracting the nonlinear buckling load associated with FG porous microbeams.

$$\nu(r)=(\nu_c-\nu_m)\left(\frac{r-Ri}{Ro-Ri}\right)^{px}+\nu_m-\frac{\eta}{2}(\nu_c+\nu_m) \tag{21a}$$

$$E(r)=E_m-\frac{\eta}{2}(E_c+E_m)+(E_c-E_m)\left(\frac{r-Ri}{Ro-Ri}\right)^{px} \tag{21b}$$

The nondimensional buckling load of microtubes with varying cross-sections is depicted in Fig. 2 for different values of μ and px, considering a functionally graded material comprising Nickel and Al_2O_3. Irrespective of their cross-sectional shapes, the buckling load demonstrates an upward trend with increasing values of μ. Notably, microtubes with uniform cross-sections exhibit notably higher buckling loads compared to other nonuniform microtubes. As the FG index is heightened, the buckling load decreases, to the extent that microtubes composed of pure ceramic display the highest buckling load. This observation sheds light on the intricate interplay between material composition, cross-sectional geometry, and mechanical behavior in microtubes, providing valuable insights into their structural stability under varying conditions.

Fig. 3 illustrates the influence of the FG parameter (η) on the nonlinear buckling load (F) of functionally graded steel/concrete microscale uniform and nonuniform pipes. These pipes are composed of a steel core coated with concrete and are subject to both pinned and clamped boundary conditions. Due to the greater stiffness of steel in comparison to concrete, an increase in the FG power index leads to an enhancement in the buckling load of both FG and BD-FG nonuniform pipes. Notably, the impact of FG parameters remains consistent for both pinned and clamped boundary conditions, highlighting a uniform trend. Additionally, uniform sections exhibit greater stability than their nonuniform counterparts. Within the realm of nonuniform cross-sections, the inherent instability of the exponential section is widely acknowledged, with the convex section demonstrating higher stability than the

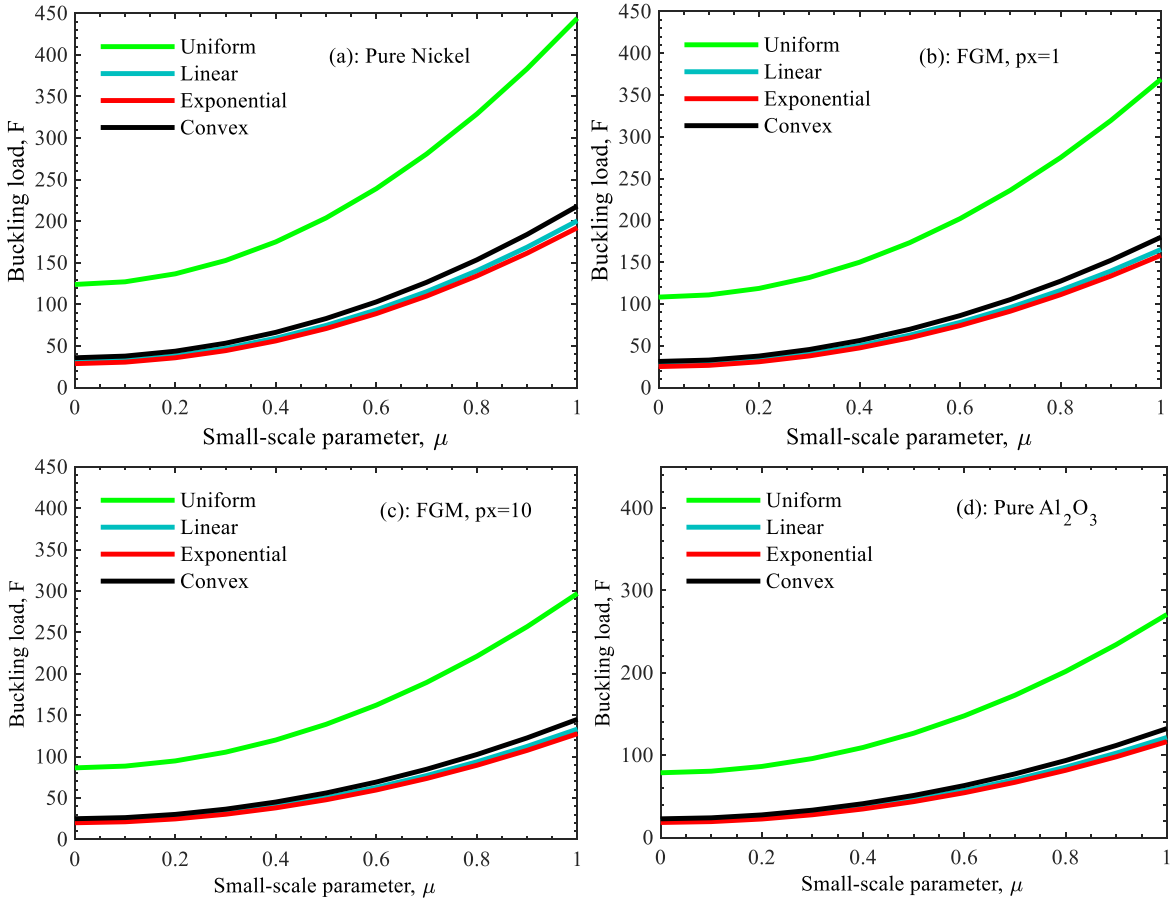

Fig. 2 Buckling load of FG (Al_2O_3/Nickel) clamped microtube with different power indices (*px*) and small-scale parameters (μ) versus multiple cross sections (W/R=1, Ro/Ri=R_L/R_R=2)

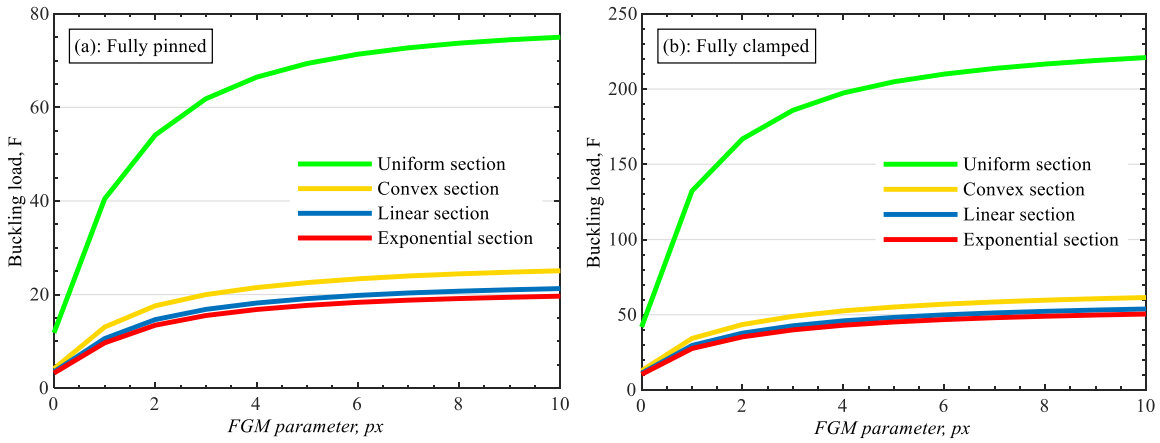

Fig. 3 The nonlinear buckling (F) behavior of bi-directional functionally graded steel/concrete pipe, versus the different FGM parameters (*px*) as well as different uniform and nonuniform cross-sections for both clamped and pinned boundary conditions, μ=0.1, W/R=1, L=40Ro_L=80Ri_L.

linear nonuniform section. These findings shed light on the intricate relationship between material composition, cross-sectional geometry, and boundary conditions, providing valuable insights into the nonlinear buckling behavior of microscale pipes in diverse scenarios.

Fig. 4 showcases an investigation into the nonlinear buckling load of imperfectly uniform and nonuniform functionally graded steel-concrete micropipes. This study explores the effects under both pinned and clamped boundary conditions, while also assessing the influence of cross-sectional variations on the nonlinear buckling loads. Across all boundary conditions and sections considered in this study, there is a consistent trend of decreasing buckling load attributed to the porosity parameter. Furthermore, as

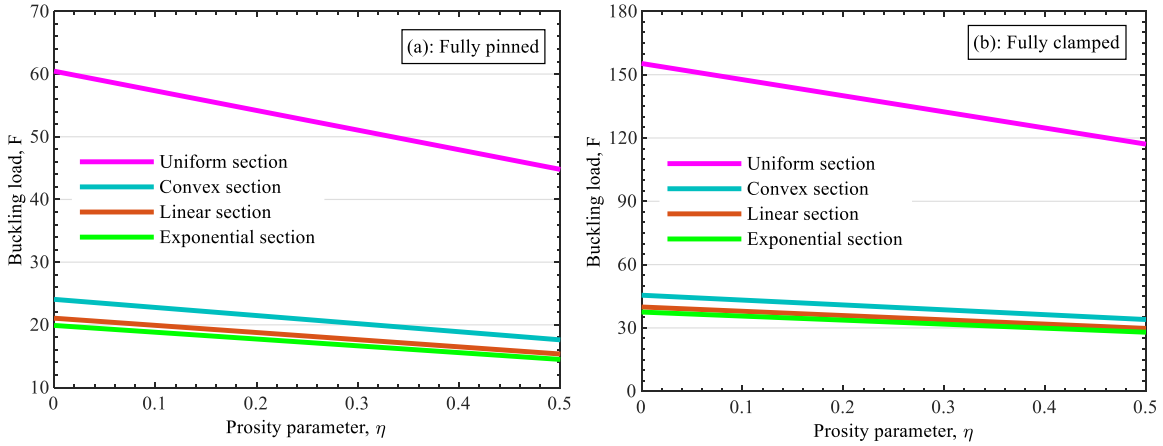

Fig. 4 Exploring the influence of porosity parameters on the nonlinear buckling load of a BD-FG steel/concrete pipe for different cross-sectional functions and various fully pinned and fully clamped boundary conditions, L=40Ro$_L$=80Ri$_L$, *px*=1, μ=0.2, W/R=2

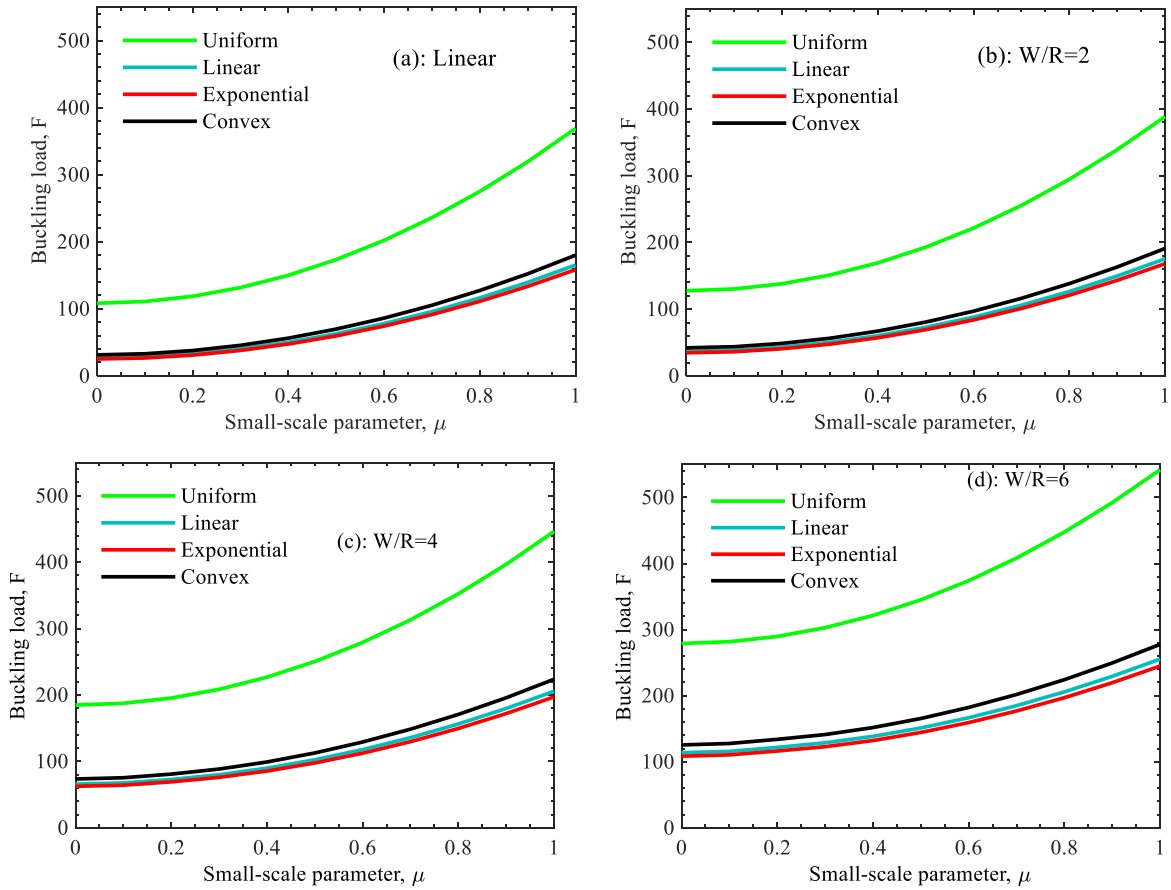

Fig. 5 Micro-sized FG (Steel/concrete) clamped tubes subjected to non-linear buckling and linear buckling at different cross sections, nonlinear amplitudes (W/R), and small-scale paarmeters (μ), Ro/Ri=R$_L$/R$_R$=2, *px*=1

depicted in Fig. 4, the observed impact of cross-sectional variations aligns with the findings presented in Fig. 3. This collective analysis contributes to a deeper understanding of the intricate interplay between boundary conditions, cross-sections, and material properties, shedding light on the nonlinear buckling behavior of functionally graded micropipes across various scenarios.

In Fig. 5, an investigation is carried out to understand the effect of significant deflection (W/R) on the buckling load of functionally graded microtubes with varying cross-sectional configurations. The visual representations within this context showcase the changes in buckling load relative to the parameter μ. Notably, the analysis reveals that the nonlinearity of the tubes contributes to an increase in the

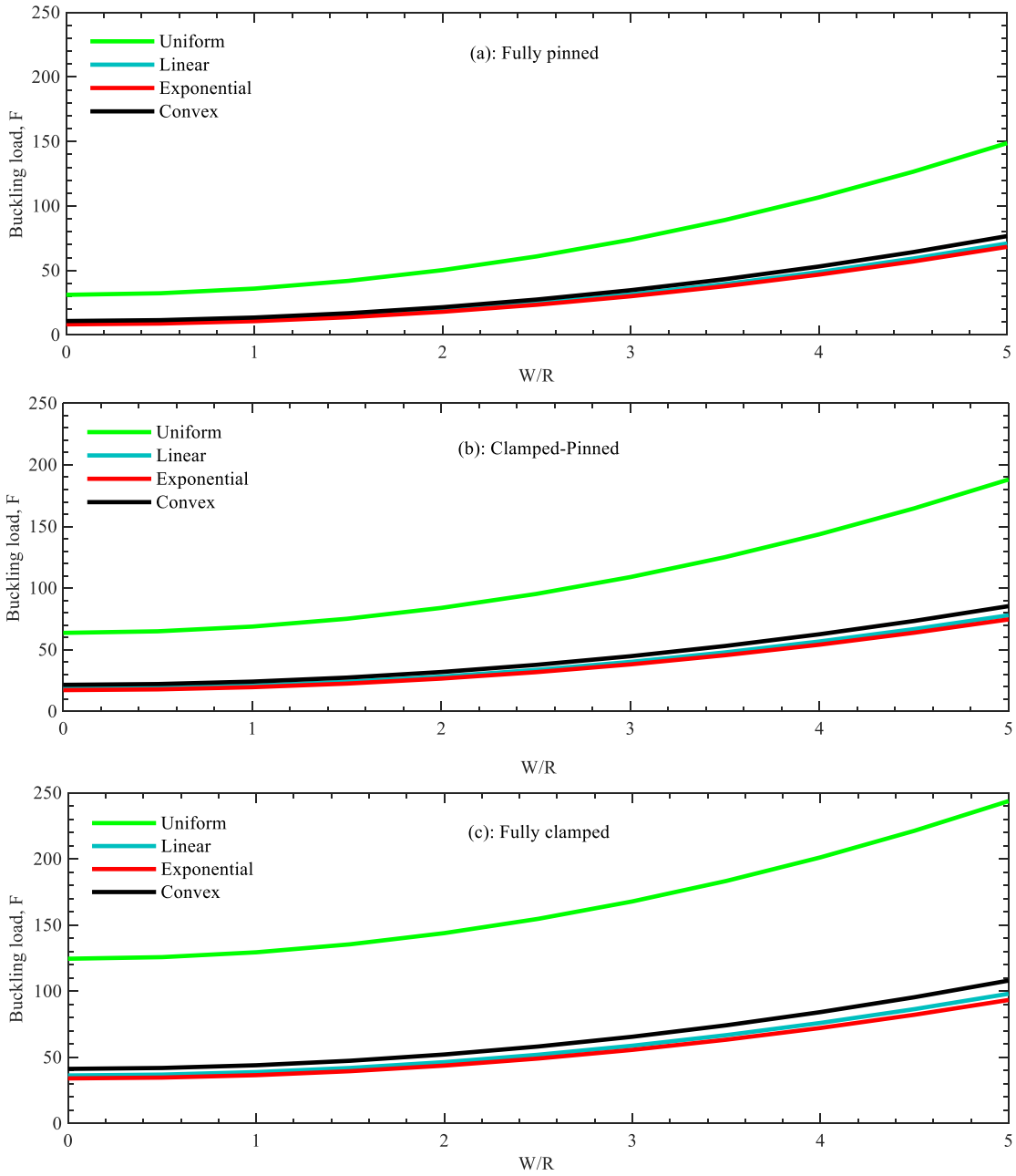

Fig. 6 Nonlinear instability threshold (F) of functionally graded (steel/concrete) tubes in relation to nonlinear deflections (W/R), considering diverse boundary conditions for linear, convex, and exponential cross-sectional profiles, Ro/Ri=R_L/R_R=2, *px*=1

buckling load. This observation suggests that the system's stability is enhanced across all types of cross-sections due to the introduction of nonlinearity.

Fig. 6 depicts the graphical representation of the system's buckling load plotted against the W/R value, considering different boundary conditions and cross-sectional geometries. It is evident from the visualization that as the influence of nonlinearity increases, the buckling load also exhibits an upward trend. Moreover, the buckling load of the microtube exhibits higher values for stiffer end conditions. Another noteworthy observation from this figure is that the use of a convex cross-section results in a higher buckling load for the microtube.

Fig. 7 displays a graphical depiction showcasing the fluctuations in the nonlinear buckling load of functionally graded microtubes. This variation is plotted against the values of the size-effect parameter, considering a range of boundary conditions and diverse cross-sectional configurations. It is evident from this figure that the microtube exhibits greater stability when the nonlocal parameter has a higher value, leading to an enhancement in the buckling load. Furthermore, it is also apparent that the system demonstrates increased stability in stiffer end conditions compared to softer end conditions.

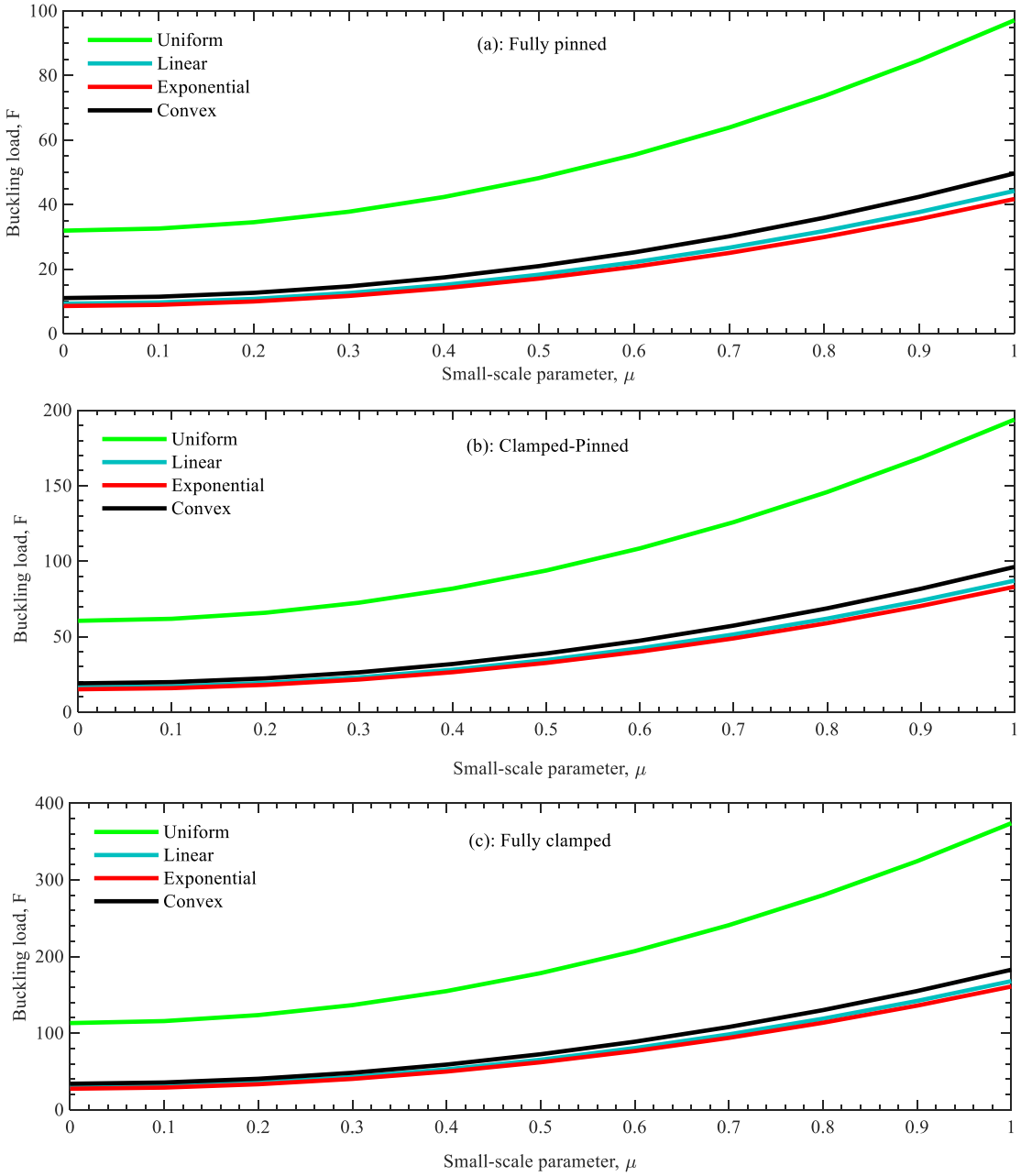

Fig. 7 Investigating size-effect and cross-section influence on nonlinear buckling of FG microtube under varying boundary conditions, Ro/Ri=R_L/R_R=2, W/R=*px*=1(Steel/concrete)

5. Conclusions

This study delved into the impact of alterations in cross-sectional geometries on both the linear and nonlinear buckling characteristics of functionally graded microbeams and bi-directional functionally graded microbeams with imperfections. To explore these effects, a combination of the modified couple stress theory, Timoshenko beam theory, and Von-Kármán nonlinear theory was employed. The investigation took into account the influence of porosity on the behavior of the beams. Several key findings emerged from this study, shedding light on the factors affecting the buckling load of FG imperfect concrete beams:

- In steel-concrete composite FG structures, an increase in FG parameters enhanced stability and elevated the buckling load, reflecting the higher stiffness of steel compared to concrete.
- Nonlinearity within the tubes contributed to higher buckling loads, indicating improved stability within the system.
- Within the framework of the modified couple stress theory, an augmentation in the small-scale parameter within the couple stress model correlated with an elevation in the buckling loads.
- Systems with more rigid boundary conditions exhibited greater stability than those with less rigid boundary conditions.

- Lower porosity values correlated with higher buckling loads and enhanced overall stability in the system design.
- Regardless of cross-sectional types and boundary conditions, in functionally graded microbeams consisting of metal coated with ceramics, reducing the FG index enhanced structural stability in the composite configuration.

References

Akgöz, B. and Civalek, Ö. (2011), "Buckling analysis of cantilever carbon nanotubes using the strain gradient elasticity and modified couple stress theories", *J. Comput. Theor. Nanosci*., **8**(9), 1821-1827. https://doi.org/10.1166/jctn.2011.1888.

Amiri Delouei, A., Emamian, A., Karimnejad, S. and Sajjadi, H. (2019a), "A closed-form solution for axisymmetric conduction in a finite functionally graded cylinder", *Int. Commun. Heat Mass Transfer*., **108**, 104280. https://doi.org/10.1016/j.icheatmasstransfer.2019.104280.

Amiri Delouei, A., Emamian, A., Karimnejad, S., Sajjadi, H. and Jing, D. (2020), "Two-dimensional analytical solution for temperature distribution in FG hollow spheres: General thermal boundary conditions", *Int. Commun. Heat Mass Transfer*., **113**, 104531. https://doi.org/10.1016/j.icheatmasstransfer.2020.104531.

Amiri Delouei, A., Emamian, A., Karimnejad, S., Sajjadi, H. and Tarokh, A. (2019b), "On 2D asymmetric heat conduction in functionally graded cylindrical segments: A general exact solution", *Int. J. Heat Mass Transfer*., **143** 118515. https://doi.org/10.1016/j.ijheatmasstransfer.2019.118515.

Azimi, M., Mirjavadi, S.S., Shafiei, N. and Hamouda, A.M.S. (2016), "Thermo-mechanical vibration of rotating axially functionally graded nonlocal Timoshenko beam", *Appl. Phys. A*., **123**(1), 104. https://doi.org/10.1007/s00339-016-0712-5.

Cai, J., Pan, J., Li, G. and Elchalakani, M. (2023), "Behaviors of eccentrically loaded ECC-encased CFST columns after fire exposure", *Eng. Struct.*, **289**, 116258. https://doi.org/10.1016/j.engstruct.2023.116258.

Cheng, F., Niu, B., Xu, N., Zhao, X. and Ahmad, A.M. (2023), "Fault detection and performance recovery design With deferred actuator replacement via a low-computation method", *IEEE T. Automat. Sci. Eng.*, 1-11. https://doi.org/10.1109/TASE.2023.3300723.

Dai, Z., Jiang, Z., Zhang, L. and Habibi, M. (2021), "Frequency characteristics and sensitivity analysis of a size-dependent laminated nanoshell", *Adv. Nano Res*., **10**(2), 175. https://doi.org/10.12989/anr.2021.10.2.175.

Dehghanbanadaki, A., Rashid, A.S.A., Ahmad, K., Yunus, N.Z.M. and Said, K.N.M. (2022), "A computational estimation model for the subgrade reaction modulus of soil improved with DCM columns", *Geomech. Eng.*, **28**(4), 385-396. https://doi.org/10.12989/gae.2022.28.4.385.

Delouei, A.A., Emamian, A., Karimnejad, S., Sajjadi, H. and Jing, D. (2020), "Asymmetric conduction in an infinite functionally graded cylinder: Two-dimensional exact analytical solution under general boundary conditions", *J. Heat Transfer*., **142**(4). https://doi.org/10.1115/1.4046306.

Ebrahimi, F., Shafiei, N., Kazemi, M. and Mousavi Abdollahi, S.M. (2017), "Thermo-mechanical vibration analysis of rotating nonlocal nanoplates applying generalized differential quadrature method", *Mech. Adv. Mater. Struct.*, **24**(15), 1257-1273. https://doi.org/10.1080/15376494.2016.1227499.

Ehyaei, J., Akbarshahi, A. and Shafiei, N. (2017), "Influence of porosity and axial preload on vibration behavior of rotating FG nanobeam", *Adv. nano Res*., **5**(2), 141-169. https://doi.org/10.12989/anr.2017.5.2.141.

Emamian, A., Amiri Delouei, A., Karimnejad, S. and Sajadi, H. (2021), "Analytical Solution of Heat Transfer in a Cone Made of Functionally Graded Material", *Amirkabir J. Mech. Eng.*, **53**(1), 539-552. https://doi.org/10.22060/mej.2019.16288.6320.

Farajpour, A., Farokhi, H. and Ghayesh, M.H. (2019), "Mechanics of fluid-conveying microtubes: Coupled buckling and post-buckling", *Vibration*, **2**(1), 102-115. https://doi.org/10.3390/vibration2010007.

Ghadiri, M., Hosseini, S.H.S. and Shafiei, N. (2016a), "A power series for vibration of a rotating nanobeam with considering thermal effect", *Mechanics of Advanced Materials and Structures*. **23**(12), 1414-1420. https://doi.org/10.1080/15376494.2015.1091527.

Ghadiri, M., Shafiei, N. and Alavi, H. (2017a), "Thermo-mechanical vibration of orthotropic cantilever and propped cantilever nanoplate using generalized differential quadrature method", *Mech. Adv. Mater. Struct*., **24**(8), 636-646. https://doi.org/10.1080/15376494.2016.1196770.

Ghadiri, M., Shafiei, N. and Alireza Mousavi, S. (2016b), "Vibration analysis of a rotating functionally graded tapered microbeam based on the modified couple stress theory by DQEM", *Appl. Phys. A*. **122**(9), 837. https://doi.org/10.1007/s00339-016-0364-5.

Ghadiri, M., Shafiei, N. and Babaei, R. (2017b), "Vibration of a rotary FG plate with consideration of thermal and Coriolis effects", *Steel Compos. Struct.*, **25**(2), 197-207. https://doi.org/10.12989/scs.2017.25.2.197.

Ghadiri, M., Shafiei, N. and Hossein Alavi, S. (2017c), "Vibration analysis of a rotating nanoplate using nonlocal elasticity theory", *J. Solid Mech*., **9**(2), 319-337. https://jsm.arak.iau.ir/article_531824_c4e4e72f55b3a3a2cde7fda2f9b20ed3.pdf.

Ghadiri, M., Shafiei, N., Salekdeh, S.H., Mottaghi, P. and Mirzaie, T. (2016c), "Investigation of the dental implant geometry effect on stress distribution at dental implant–bone interface", *J. Braz. Soc. Mech. Sci. Eng*., **38**(2), 335-343. https://doi.org/10.1007/s40430-015-0472-8.

Ghannadpour, S.A.M. and Mohammadi, B. (2010), "Buckling analysis of micro- and nano-rods/tubes based on nonlocal timoshenko beam theory using chebyshev polynomials", *Adv. Mater. Res.*, **123-125** 619-622. https://doi.org/10.4028/www.scientific.net/AMR.123-125.619.

Guo, J., Baharvand, A., Tazeddinova, D., Habibi, M., Safarpour, H., Roco-Videla, A. and Selmi, A. (2021), "An intelligent computer method for vibration responses of the spinning multi-layer symmetric nanosystem using multi-physics modeling", *Eng. with Comput*., 1-22. https://doi.org/10.1007/s00366-021-01433-4.

Guo, S., Zhao, X., Wang, H. and Xu, N. (2023), "Distributed consensus of heterogeneous switched nonlinear multiagent systems with input quantization and DoS attacks", *Appl. Math. Comput*., **456,** 128127. https://doi.org/10.1016/j.amc.2023.128127.

Hayati, Y. and Eskandari-Ghadi, M. (2018), "Three-dimensional coupled thermoelastodynamic stress and flux induced wave propagation for isotropic half-space with scalar potential functions", *Zeitschrift für angewandte Mathematik und Physik*. **69**(1), 1-32. https://doi.org/10.1007/s00033-018-0910-4.

Hayati, Y., Eskandari-Ghadi, M., Raoofian, M., Rahimian, M. and Ardalan, A.A. (2013), "Dynamic Green's functions of an axisymmetric thermoelastic half-space by a method of potentials", *J. Eng. Mech.*, **139**(9), 1166-1177. https://doi.org/10.1061/(ASCE)EM.1943-7889.0000540.

Hayati, Y., Eslami, A. and Havaei, G. (2021), "Asymmetric 3D stress-and flux-induced wave propagation in transversely

isotropic thermoelastic solids by using of analytical methods", *Waves in Random and Complex Media*. 1-18. https://doi.org/10.1080/17455030.2021.2000671.

He, F., Amiri Delouei, A., Ellahi, R., Alamri, S.Z., Emamian, A. and Ghorbani, S. (2023), "Unsteady temperature distribution in a cylinder made of functionally graded materials under circumferentially-varying convective heat transfer boundary conditions", https://doi.org/10.1515/zna-2023-0039.

He, Y. and Cai, Y. (2021), "Influence of cross-section on the linear and nonlinear buckling analysis of imperfect functionally graded micro-tubes", *Mech. Based Des. Struct. Machines*, 1-22. https://doi.org/10.1080/15397734.2021.1956330.

Hou, F., Wu, S., Moradi, Z. and Shafiei, N. (2021a), "The computational modeling for the static analysis of axially functionally graded micro-cylindrical imperfect beam applying the computer simulation", *Eng. with Comput*., https://doi.org/10.1007/s00366-021-01456-x.

Hou, F., Wu, S., Moradi, Z. and Shafiei, N. (2021b), "The computational modeling for the static analysis of axially functionally graded micro-cylindrical imperfect beam applying the computer simulation", *Eng. with Comput*., 1-19. https://doi.org/10.1007/s00366-021-01456-x.

Huang, H., Yao, Y., Zhang, W. and zhou, L. (2023a), "A push-out test on partially encased composite column with different positions of shear studs", *Eng. Struct.*, **289**, 116343. https://doi.org/10.1016/j.engstruct.2023.116343.

Huang, S., Zong, G., Wang, H., Zhao, X. and Alharbi, K.H. (2023b), "Command filter-based adaptive fuzzy self-triggered control for MIMO nonlinear systems with time-varying full-state constraints", *Int. J. Fuzzy Syst.*, https://doi.org/10.1007/s40815-023-01560-8.

Huang, X., Zhang, Y., Moradi, Z. and Shafiei, N. (2021), "Computer simulation via a couple of homotopy perturbation methods and the generalized differential quadrature method for nonlinear vibration of functionally graded non-uniform micro-tube", *Eng. with Comput.*, 1-18. https://doi.org/10.1007/s00366-021-01395-7.

Huang, Y., Zhang, M. and Rong, H. (2016), "Buckling analysis of axially functionally graded and non-uniform beams based on timoshenko theory", *Acta Mechanica Solida Sinica*. **29**(2), 200-207. https://doi.org/10.1016/S0894-9166(16)30108-2.

Jiao, P., Borchani, W., Hasni, H., Alavi, A.H. and Lajnef, N. (2016), "Post-buckling response of non-uniform cross-section bilaterally constrained beams", *Mech. Res. Commun.*, **78**, 42-50. https://doi.org/10.1016/j.mechrescom.2016.09.012.

Kabir, A.M.R., Inoue, D., Afrin, T., Mayama, H., Sada, K. and Kakugo, A. (2015), "Buckling of Microtubules on a 2D Elastic Medium", *Scientific Reports*. **5**(1), 17222. https://doi.org/10.1038/srep17222.

Kim, J., Żur, K.K. and Reddy, J.N. (2019), "Bending, free vibration, and buckling of modified couples stress-based functionally graded porous micro-plates", *Compos. Struct.*, **209**, 879-888. https://doi.org/10.1016/j.compstruct.2018.11.023.

Li, D., Nie, J.H., Wang, H., Yan, J.B., Hu, C.X. and Shen, P. (2023a), "Damage location, quantification and characterization of steel-concrete composite beams using acoustic emission", *Eng. Struct.*, **283**, 115866. https://doi.org/10.1016/j.engstruct.2023.115866.

Li, J., Liu, Y. and Lin, G. (2023b), "Implementation of a coupled FEM-SBFEM for soil-structure interaction analysis of large-scale 3D base-isolated nuclear structures", *Comput. Geotech.*, **162** 105669. https://doi.org/10.1016/j.compgeo.2023.105669.

Li, L. and Hu, Y. (2015), "Buckling analysis of size-dependent nonlinear beams based on a nonlocal strain gradient theory", *Int. J. Eng. Sci*., **97**, 84-94. https://doi.org/10.1016/j.ijengsci.2015.08.013.

Li, Z.Z., Zhu, T., Xiao, S.N., Zhang, J.K., Wang, X.R. and Ding, H.X. (2023c), "Simulation method for train curve derailment collision and the effect of curve radius on collision response", *Proceedings of the Institution of Mechanical Engineers, Part F: Journal of Rail and Rapid Transit*. 09544097231154313. https://doi.org/10.1177/09544097231154313.

Liu, Z., Su, S., Xi, D. and Habibi, M. (2020), "Vibrational responses of a MHC viscoelastic thick annular plate in thermal environment using GDQ method", *Mech. Based Des. Struc*., 1-26. https://doi.org/10.1080/15397734.2020.1784201.

Mohammadi, A., Ebadi, T. and Boroomand, M.R. (2020), "Interface shear between different oil-contaminated sand and construction materials", *Geomech. Eng*., **20**(4), 299-312. https://doi.org/10.12989/gae.2020.20.4.299.

Mousavi, S.M., Shafiei, N. and Dadvand, A. (2017), "Numerical simulation of subsonic turbulent flow over NACA0012 airfoil: evaluation of turbulence models", *Sigma J. Eng. Nat. Sci.*, **35**(1), 133-155. https://dergipark.org.tr/en/pub/sigma/issue/65585/1016455.

Naeeni, M.R., Eskandari-Ghadi, M., Ardalan, A., Pak, R., Rahimian, M. and Hayati, Y. (2015), "Coupled thermoviscoelastodynamic Green's functions for bi-material half-space", *ZAMM-J. Appl Math. Mechanics/Zeitschrift für Angewandte Mathematik und Mechanik*. **95**(3), 260-282. https://doi.org/10.1002/zamm.201200135.

Omidi, S., Oskooee, M.B. and Shafiei, N. (2013), "Finite element analysis of an ultra-fine grained Titanium dental implant covered by different thicknesses of hydroxyapatite layer", *Indian J. Dentistry*, **4**(1), 1-4. https://doi.org/10.1016/j.ijd.2012.10.002.

Raoofian Naeeni, M., Eskandari-Ghadi, M., Ardalan, A.A., Rahimian, M. and Hayati, Y. (2013), "Analytical solution of coupled thermoelastic axisymmetric transient waves in a transversely isotropic half-space", *J. Appl. Mech.*, **80**(2). https://doi.org/10.1115/1.4007786.

Shafiei, N., Ghadiri, M., Makvandi, H. and Hosseini, S.A. (2017), "Vibration analysis of Nano-Rotor's Blade applying Eringen nonlocal elasticity and generalized differential quadrature method", *Appl. Math. Model.*, **43**, 191-206. https://doi.org/10.1016/j.apm.2016.10.061.

Shafiei, N., Hamisi, M. and Ghadiri, M. (2020), "Vibration analysis of rotary tapered axially functionally graded timoshenko nanobeam in thermal environment", *J. Solid Mech.*, **12**(1), 16-32. https://doi.org/10.22034/jsm.2019.563759.1273.

Shafiei, N. and Kazemi, M. (2017), "Nonlinear buckling of functionally graded nano-/micro-scaled porous beams", *Compos. Struct.*, **178** 483-492. https://doi.org/10.1016/j.compstruct.2017.07.045.

Shafiei, N., Kazemi, M. and Ghadiri, M. (2016), "Nonlinear vibration behavior of a rotating nanobeam under thermal stress using Eringen's nonlocal elasticity and DQM", *Appl. Phys. A*. **122**(8), 728. https://doi.org/10.1007/s00339-016-0245-y.

Shahabinejad, E., Shafiei, N. and Ghadiri, M. (2018), "Influence of temperature change on modal analysis of rotary functionally graded nano-beam in thermal environment", *J. Solid Mech*., **10**(4), 779-803. https://jsm.arak.iau.ir/article_545719.html.

Shao, Y., Zhao, Y., Gao, J. and Habibi, M. (2021), "Energy absorption of the strengthened viscoelastic multi-curved composite panel under friction force", *Arch. Civil Mech. Eng*., **21**(4), 1-29. https://doi.org/10.1007/s43452-021-00279-3.

Shivanian, E., Ghadiri, M. and Shafiei, N. (2017), "Influence of size effect on flapwise vibration behavior of rotary microbeam and its analysis through spectral meshless radial point interpolation", *Appl. Phys. A*., **123**(5), 329. https://doi.org/10.1007/s00339-017-0955-9.

Tahmasebinia, F., Yip, C.S., Lok, C.F., Sun, Y., Wu, J., Sepasgozar, S.M.E. and Marroquin, F.A. (2022), *Dynamic Behavior of the Composite Steel–Concrete Beam Floor Systems under*

Free and Forced Vibration,

Tang, F., Wang, H., Zhang, L., Xu, N. and Ahmad, A.M. (2023), "Adaptive optimized consensus control for a class of nonlinear multi-agent systems with asymmetric input saturation constraints and hybrid faults", *Commun. Nonlinear Sci. Numer. Simul.*, **126**, 107446. https://doi.org/10.1016/j.cnsns.2023.107446.

Ugurlu, O.F. and Ozturk, C.A. (2021), "Experimental investigation for the use of tailings as paste-fill material through design of experiment", *Geomech. Eng.*, **26**(5), 465. https://doi.org/10.12989/gae.2021.26.5.465.

Wang, H., Zhang, X. and Wang, M. (2023a), "Rapid texture depth detection method considering pavement deformation calibration", *Measurement*, **217**, 113024. https://doi.org/10.1016/j.measurement.2023.113024.

Wang, P., Gao, Z., Pan, F., Moradi, Z., Mahmoudi, T. and Khadimallah, M.A. (2022), "A couple of GDQM and iteration techniques for the linear and nonlinear buckling of bi-directional functionally graded nanotubes based on the nonlocal strain gradient theory and high-order beam theory", *Eng. Anal. Bound. Elem.*, **143**, 124-136. https://doi.org/10.1016/j.enganabound.2022.06.007.

Wang, T., Zhou, G., Wang, J. and Wang, D. (2020a), "Impact of spatial variability of geotechnical properties on uncertain settlement of frozen soil foundation around an oil pipeline", *Geomech. Eng.*, **20**(1), 19-28. https://doi.org/10.12989/gae.2020.20.1.019.

Wang, Y., Jia, Q. and Deng, T. (2023b), "The role of nanotechnology in reducing the impact on the ball and increasing the speed of its movement", *Geomech. Eng.*, **32**(5), 463-474. https://doi.org/10.12989/gae.2023.32.5.463.

Wang, Z., Yu, S., Xiao, Z. and Habibi, M. (2020b), "Frequency and buckling responses of a high-speed rotating fiber metal laminated cantilevered microdisk", *Mech. Adv. Mater. Struct.*, 1-14. https://doi.org/10.1080/15376494.2020.1824284.

Wu, J. and Habibi, M. (2021), "Dynamic simulation of the ultra-fast-rotating sandwich cantilever disk via finite element and semi-numerical methods", *Eng. with Comput.,* 1-17. https://doi.org/10.1007/s00366-021-01396-6.

Wu, M., Ba, Z. and Liang, J. (2022), "A procedure for 3D simulation of seismic wave propagation considering source-path-site effects: Theory, verification and application", *Earthq. Eng. Struct. D.*, **51**(12), 2925-2955. https://doi.org/10.1002/eqe.3708.

Wu, W., Xu, N., Niu, B., Zhao, X. and Ahmad, A.M. (2023a), *Low-Computation Adaptive Saturated Self-Triggered Tracking Control of Uncertain Networked Systems*,

Wu, Z., Huang, B., Fan, J. and Chen, H. (2023b), "Homotopy based stochastic finite element model updating with correlated static measurement data", *Measurement*, **210**, 112512. https://doi.org/10.1016/j.measurement.2023.112512.

Xiang, P. and Liew, K.M. (2011), "Predicting buckling behavior of microtubules based on an atomistic-continuum model", *Int. J. Solids Struct.*, **48**(11), 1730-1737. https://doi.org/10.1016/j.ijsolstr.2011.02.022.

Xu, W., Pan, G., Moradi, Z. and Shafiei, N. (2021), "Nonlinear forced vibration analysis of functionally graded non-uniform cylindrical microbeams applying the semi-analytical solution", *Compos. Struct.*, 114395. https://doi.org/10.1016/j.compstruct.2021.114395.

Yang, F., Chong, A.C.M., Lam, D.C.C. and Tong, P. (2002), "Couple stress based strain gradient theory for elasticity", *Int. J. Solids Struct.*, **39**(10), 2731-2743. https://doi.org/10.1016/S0020-7683(02)00152-X.

Yang, J. and Shen, H.S. (2002), "Vibration characteristics and transient response of shear-deformable functionally graded plates in thermal environments", *J. Sound Vib.*, **255**(3), 579-602. https://doi.org/10.1006/jsvi.2001.4161.

Yang, K., Guan, J., Numata, K., Wu, C., Wu, S., Shao, Z. and Ritchie, R.O. (2019), "Integrating tough Antheraea pernyi silk and strong carbon fibres for impact-critical structural composites", *Nature Commun.*, **10**(1), 3786. https://doi.org/10.1038/s41467-019-11520-2.

Yang, Y., Lin, B. and Zhang, W. (2023), "Experimental and numerical investigation of an arch–beam joint for an arch bridge", *Arch. Civil Mech. Eng.*, **23**(2), 101. https://doi.org/10.1007/s43452-023-00645-3.

Yang, Z., Xu, J., Feng, Q., Liu, W., He, P. and Fu, S. (2022), "Elastoplastic analytical solution for the stress and deformation of the surrounding rock in cold region tunnels considering the influence of the temperature field", *Int. J. Geomech.*, **22**(8), 04022118. https://doi.org/10.1061/(ASCE)GM.1943-5622.0002466.

Yao, Y., Zhou, L., Huang, H., Chen, Z. and Ye, Y. (2023), "Cyclic performance of novel composite beam-to-column connections with reduced beam section fuse elements", *Structures*, **50**, 842-858. https://doi.org/10.1016/j.istruc.2023.02.054.

Yu, H., Zhang, J., Fang, M., Ma, T., Wang, B., Zhang, Z., Hu, Z., Li, H., Cao, X., Ding, C., Deng, H. and Yang, K. (2023), "Bio-inspired strip-shaped composite composed of glass fabric and waste selvedge from A. pernyi silk for lightweight and high-impact applications", *Compos. Part A: Appl. Sci. Manufact.*, **174** 107715. https://doi.org/10.1016/j.compositesa.2023.107715.

Zhang, C. (2023), "The active rotary inertia driver system for flutter vibration control of bridges and various promising applications", *Science China Technol. Sci.*, **66**(2), 390-405. https://doi.org/10.1007/s11431-022-2228-0.

Zhao, Y., Niu, B., Zong, G., Zhao, X. and Alharbi, K.H. (2023), "Neural network-based adaptive optimal containment control for non-affine nonlinear multi-agent systems within an identifier-actor-critic framework", *J. Franklin Inst.*, **360**(12), 8118-8143. https://doi.org/10.1016/j.jfranklin.2023.06.014.

Zhou, C., Zhao, Y., Zhang, J., Fang, Y. and Habibi, M. (2020), "Vibrational characteristics of multi-phase nanocomposite reinforced circular/annular system", *Adv. Nano Res.*, **9**(4), 295-307. https://doi.org/10.12989/anr.2020.9.4.295.

Zhou, F., Jiang, H., Huang, L., Hu, Y., Xie, Z., Zeng, Z., Liu, M., Wang, B. and Zhou, X. (2023), *Early Shrinkage Modeling of Complex Internally Confined Concrete Based on Capillary Tension Theory.*

CC